GPS/INS Integration for Vehicle Navigation based on INS Error Analysis in Kalman Filtering

M. R.Emami Shaker [1], A.Ghaffari[2], A.Maghsoodpour[3], A. Khodayari[4]

1. M.Sc. Student, Mechanical Engineering Department, Science and Research Branch, Islamic Azad University, Tehran, Iran
2. Professor, Mechanical Engineering Department, K.N.Toosi University of Technology, Tehran, Iran
3. Assistant Professor, Mechanical Engineering Department, Science and Research Branch, Islamic Azad University, Tehran, Iran
4. Associate Professor, Mechanical Engineering Department, Pardis Branch, Islamic Azad University, Tehran, Iran
[*] *arkhodayari@yahoo.com*

Abstract

The Global Positioning System (GPS) and an Inertial Navigation System (INS) are two basic navigation systems. Due to their complementary characters in many aspects, a GPS/INS integrated navigation system has been a hot research topic in the recent decade. The Micro Electrical Mechanical Sensors (MEMS) successfully solved the problems of price, size and weight with the traditional INS. Therefore they are commonly applied in GPS/INS integrated systems. The biggest problem of MEMS is the large sensor errors, which rapidly degrade the navigation performance in an exponential speed. Three levels of GPS/IMU integration structures, i.e. loose, tight and ultra tight GPS/IMU navigation, are proposed by researchers. The loose integration principles are given with detailed equations as well as the basic INS navigation principles. The Extended Kalman Filter (EKF) is introduced as the basic data fusion algorithm, which is also the core of the whole navigation system to be presented. The kinematic constraints of land vehicle navigation, i.e. velocity constraint and height constraint, are presented. A detailed implementation process of the GPS/IMU integration system is given. Based on the system model, we show the propagation of position standard errors with the tight integration structure under different scenarios. A real test with loose integration structure is carried out, and the EKF performances as well as the physical constraints are analyzed in detail.

Keywords: *GPS/INS Integration, Vehicle Navigation, INS Error Analysis, Kalman Filtering.*

1. Introduction

Inertial Navigation Systems (INS) utilize inertial sensors to provide navigation information continuously with time [1]. In a Strapdown 3D INS with full Inertial Measurements Unit (IMU) [2], three acceleration sensors (Accelerometers) and three angular rate sensors (Gyroscopes) are utilized. The accelerometers measure the acceleration of the moving body in three orthogonal directions. Gyroscope measures the rotation rate around these three basic orthogonal axes. The essential functions in INS are defined as follows: 1) Determination of the angular motion of a vehicle using gyroscopic sensors, from which its attitude relative to a reference frame may be derived. 2) Measure the acceleration using accelerometers. 3) Resolve the acceleration measurements into the reference frame using the knowledge of attitude. 4) Account for the gravity component. 5) Integrate the resolved accelerations to estimate the velocity and position of the vehicle. Although INS systems have good short term accuracy, there are two main problems in using such a scheme. The first problem is the sensor imperfections and drifts [3]. The second problem is that the measurements of such sensors must be mathematically integrated to provide velocity, position, and attitude information. Integration causes errors to accumulate [4] resulting in huge drifts over time that growth without bounds. On the other side, GPS systems provide consistent long term accuracy giving position and velocity updates using GPS satellites signals processing [5]. A major problem of GPS is signal blockage and multi-path in urban canyons, under buildings, and tunnels. In these environments, signal may be difficult to acquire or number of satellites available may be not sufficient to provide position information [6]. Based on the complementary error characteristics of INS and GPS, an integrated solution using both systems is often used. Although there are many approaches to fuse data from both systems, KF is most widely used [7].

[DOI: 10.22068/ijae.7.4.2562]

KF utilizes an error dynamic model of the INS system errors to implement two main steps: Prediction step and Update step. Prediction step is done as long as no GPS update is available. In this step, the system uses the error dynamic model to estimate the INS errors. In the update step, GPS velocity and position measurements are used to get optimal estimate of INS errors. Thus, by subtracting INS errors from the INS output, accurate navigation information is obtained. This integration scheme is called loosely coupled which is utilized here in this work. This scheme is shown in Fig. 1.

2. MEMS-based INS

The strapdown inertial navigation system (INS) involves mechanization equations, which are the numerical tool to implement the physical phenomenon that relates the inertial sensor measurements to the navigation state (i.e., position, velocity and attitude) [8, 9]. The shaded rectangle in Figure 2 represents the INS mechanization equations that can describe the motion of a vehicle, taking as input the inertial measures in the body frame (accelerations and angular rotations) and converting these measurements into a reference frame for navigation. In this case, it provides position, velocity and attitude of the vehicle with respect to the North-East-Down (NED) local geodetic frame.

The inertial measurement unit (IMU), which is part of the INS, is the device where the inertial sensors are mounted; it provides the accelerations and angular rotations along three orthogonal directions with respect to the body frame (Figure 2). In a low-cost INS (MEMS grade), the measurement of these accelerometer and gyro sensors is affected by different errors, which can be classified as deterministic and stochastic errors. Figure 3 depicts some of these errors through a simple relationship between IMU physical signal and the sensor output.

Deterministic errors are due to manufacturing and mounting defects and can be calibrated out from the data; on the other hand, the stochastic errors are the random errors that occur due to random variations of bias or scale factor over time [10]. There are several errors that affect the inertial sensors: the misalignment errors are the result of non-orthogonalities of the sensor axes and are usually treated as deterministic error. The scale factor represents the sensibility of the sensor, and it is the result of manufacturing tolerances or aging; it is usually divided between a linear and a non-linear part, where the linear part is obtained from calibration, while the non-linear is modeled with a stochastic process [11]. In the case of the bias, it is divided between bias turn-on and bias-drift: the bias turn-on is constant, but it varies from turn-on to turn-on and is considered as a deterministic error; the bias-drift presents a random behavior and needs to be modeled with a stochastic process [12, 13]. Regarding the random error (Figure 2), this is an additional signal resulting from noise of the sensor itself or other components that interfere with the signal provided by the sensor; it is also considered as part of the stochastic error of the sensor. The deterministic errors can be minimized before implementing the mechanization equations by following different procedures through laboratory calibrations. In this work, we focused on the stochastic error, specifically, in the bias-drift, since the stochastic modeling of this error is a challenging task, not only because of the random nature, but also because it seriously affects the performance of a navigation system. Therefore, a suitable estimation of the stochastic model parameters of this error will improve the performance of the INS; as a consequence, the input error to the mechanization stage (Figure 1) can be compensated and, in turn, the position error minimized.

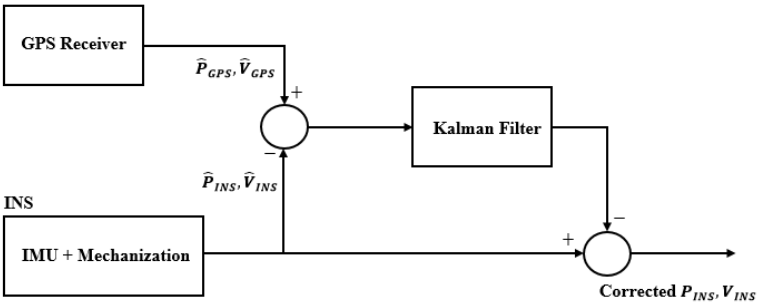

Fig1. INS/GPS Integration in Loosely Coupled scheme

[DOI: 10.22068/ijae.7.4.2562]

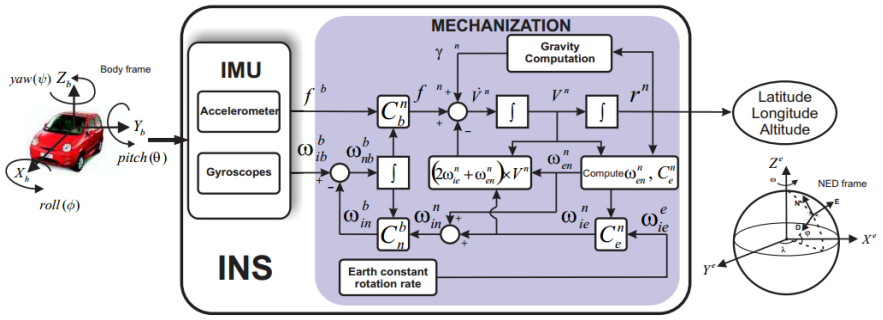

Fig2. Navigation frame inertial navigation system (INS) mechanization; figure kindly taken from [14].

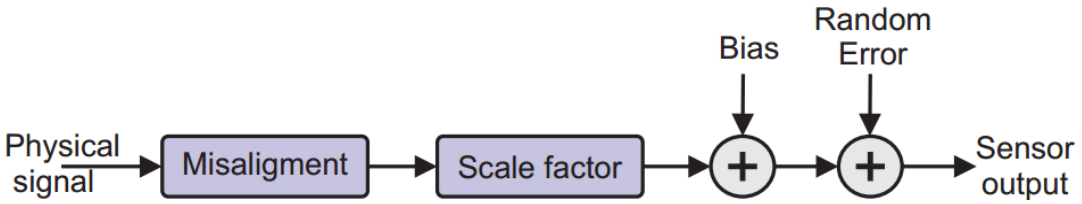

Fig3. Inertial sensor error modeling; figure kindly taken from [15].

3. Perturbation of the Navigation Equation

The error analysis in this paper utilizes perturbation methods to linearize the nonlinear system differential equations. For example, the perturbation of the position, velocity and attitude DCM can be expressed as:

$$\hat{\boldsymbol{r}}^n = \boldsymbol{r}^n + \delta\boldsymbol{r}^n \quad (1)$$

$$\hat{\boldsymbol{V}}^n = \boldsymbol{V}^n + \delta\boldsymbol{V}^n \quad (2)$$

$$\hat{\boldsymbol{C}}_b^n = (\boldsymbol{I} - \boldsymbol{E}^n)\boldsymbol{C}_b^n \quad (3)$$

Where, e.g. $\hat{\boldsymbol{V}}^n$ is computed velocity, $\boldsymbol{V}^n$ is true velocity and $\delta\boldsymbol{V}^n$ is computed velocity error. Also $\boldsymbol{E}^n$ is the skew symmetric form of the attitude errors:

$$\boldsymbol{E}^n = \begin{bmatrix} 0 & -\epsilon_D & \epsilon_E \\ \epsilon_D & 0 & -\epsilon_N \\ -\epsilon_E & \epsilon_N & 0 \end{bmatrix} \quad (4)$$

Using above equations, the state vector can be defined as (5):

$$\mathbf{X} = [\delta\boldsymbol{r}^n \quad \delta\boldsymbol{V}^n \quad \boldsymbol{\epsilon}^n] \quad (5)$$

Where $\delta\boldsymbol{r}^n$ is the position error vector, $\delta\boldsymbol{V}^n$ is the velocity error vector and $\boldsymbol{E}^n$ is the attitude error vector.

3.1. Position Error Equation

The position error dynamics equation can be obtained using the partial derivatives, because the position equations are a function of position and velocity.

$$\delta\dot{\boldsymbol{r}}^n = \boldsymbol{F}_{rr}\delta\boldsymbol{r}^n + \boldsymbol{F}_{rv}\delta\boldsymbol{v}^n \quad (6)$$

Where

$$\boldsymbol{F}_{er} = \begin{bmatrix} -\omega_e \sin\varphi & 0 & \frac{-v_E}{(N+h)^2} \\ 0 & 0 & \frac{v_N}{(M+h)^2} \\ -\omega_e \cos\varphi - \frac{v_E}{(N+h)\cos^2\varphi} & 0 & \frac{v_E \tan\varphi}{(N+h)^2} \end{bmatrix} \quad (7)$$

$$\boldsymbol{F}_{ev} = \begin{bmatrix} 0 & \frac{1}{N+h} & 0 \\ \frac{-1}{M+h} & 0 & 0 \\ 0 & \frac{-\tan\varphi}{N+h} & 0 \end{bmatrix} \quad (8)$$

Where, M and N, the radii curvature in the meridian and prime vertical are considered as constants.

3.2. Velocity Error Equation

The computed version of velocity can be obtained as (9).

$$\dot{\hat{\boldsymbol{v}}}^n = \hat{\boldsymbol{C}}_b^n \tilde{\boldsymbol{f}}^b - (2\hat{\boldsymbol{\omega}}_{ie}^n + \hat{\boldsymbol{\omega}}_{en}^n) \times \hat{\boldsymbol{v}}^n + \boldsymbol{g}^n \quad (9)$$

The velocity error dynamics can be written as (10).

$$\delta\dot{\boldsymbol{V}}^n = \boldsymbol{F}_{vr}\delta\boldsymbol{r}^n + \boldsymbol{F}_{vv}\delta\boldsymbol{v}^n + (\boldsymbol{f}^n \times)\boldsymbol{\epsilon}^n + \boldsymbol{C}_b^n\,\delta\boldsymbol{f}^b \quad (10)$$

Where:

[DOI: 10.22068/ijae.7.4.2562]

$$\boldsymbol{F}_{vr} = \begin{bmatrix} -2v_E\omega_e\cos\varphi - \frac{v_E^2}{(N+h)\cos^2\varphi} & 0 & \frac{-v_D v_N}{(M+h)^2} + \frac{v_E^2\tan\varphi}{(N+h)^2} \\ 2\omega_e(v_N\cos\varphi - v_D\sin\varphi) + \frac{v_E v_N}{(N+h)\cos^2\varphi} & 0 & \frac{-v_E v_N}{(N+h)^2} - \frac{v_E v_N\tan\varphi}{(N+h)^2} \\ 2v_E\omega_e\sin\varphi & 0 & \frac{v_E^2}{(N+h)^2} + \frac{v_N^2}{(M+h)^2} - \frac{2g}{(R+h)} \end{bmatrix} \quad (11)$$

$$F_{vv} = \begin{bmatrix} \frac{v_D}{(M+h)} & -2\omega_e\sin\varphi - 2\frac{v_E\tan\varphi}{(N+h)} & \frac{v_N}{(M+h)} \\ 2\omega_e\sin\varphi + \frac{v_E\tan\varphi}{(N+h)} & \frac{v_D + v_N\tan\varphi}{(N+h)} & 2\omega_e\cos\varphi + \frac{v_E}{(N+h)} \\ -2\frac{v_N}{(M+h)} & -2\omega_e\cos\varphi - 2\frac{v_E}{(N+h)} & 0 \end{bmatrix} \quad (12)$$

3.3 Attitude Error Equation

The attitude error dynamics can be written as (13).

$$\dot{\boldsymbol{\epsilon}}^n = \boldsymbol{F}_{er}\delta\boldsymbol{r}^n + \boldsymbol{F}_{ev}\delta\boldsymbol{v}^n - (\boldsymbol{\omega}_{in}^n\times)\boldsymbol{\epsilon}^n - \boldsymbol{C}_b^n\,\delta\boldsymbol{\omega}_{ib}^b \quad (13)$$

where

$$\boldsymbol{F}_{er} = \begin{bmatrix} -\omega_e\sin\varphi & 0 & \frac{-v_E}{(N+h)^2} \\ 0 & 0 & \frac{v_N}{(M+h)^2} \\ -\omega_e\cos\varphi - \frac{v_E}{(N+h)\cos^2\varphi} & 0 & \frac{v_E\tan\varphi}{(N+h)^2} \end{bmatrix} \quad (14)$$

$$\boldsymbol{F}_{ev} = \begin{bmatrix} 0 & \frac{1}{N+h} & 0 \\ \frac{-1}{M+h} & 0 & 0 \\ 0 & \frac{-\tan\varphi}{N+h} & 0 \end{bmatrix} \quad (15)$$

3.4. Continuous INS Error Dynamics

The final, continuous error model can be constructed as (16).

$$\dot{\mathbf{x}} = \mathbf{F}\mathbf{x} + \mathbf{G}\mathbf{u} \quad (16)$$

Where $\boldsymbol{F}$ is the dynamic matrix, $\boldsymbol{x}$ is the state vector, $\boldsymbol{G}$ is the design matrix and $\boldsymbol{u}$ is the forcing vector function.

$$\mathbf{F} = \begin{bmatrix} \boldsymbol{F}_{rr} & \boldsymbol{F}_{rv} & 0 \\ \boldsymbol{F}_{vr} & \boldsymbol{F}_{vv} & (\mathbf{f}^n\times) \\ \boldsymbol{F}_{er} & \boldsymbol{F}_{ev} & -(\boldsymbol{\omega}_{in}^n\times) \end{bmatrix} \quad (17)$$

$$\mathbf{x} = \begin{bmatrix} \delta\boldsymbol{r}^n \\ \delta\boldsymbol{v}^n \\ \boldsymbol{\epsilon}^n \end{bmatrix} \quad (18)$$

$$\mathbf{G} = \begin{bmatrix} 0 & 0 \\ \boldsymbol{C}_b^n & 0 \\ 0 & -\boldsymbol{C}_b^n \end{bmatrix} \quad (19)$$

$$\mathbf{u} = \begin{bmatrix} \delta\mathbf{f}^n \\ \delta\boldsymbol{\omega}_{ib}^b \end{bmatrix} \quad (20)$$

The specific force, $\mathbf{f}^n$, is the sensed output of the accelerometer transformed into the navigation frame. The specific force is a combination of internal and gravitational accelerations:

$$\mathbf{f}^n = \boldsymbol{C}_i^n\ddot{\boldsymbol{r}}^i - \boldsymbol{g} \quad (21)$$

Where $\boldsymbol{g}$ is the gravitational acceleration. The specific force vector is defined as

$$\mathbf{f}^n = \begin{bmatrix} f_N \\ f_E \\ f_D \end{bmatrix} = \begin{bmatrix} \dot{v}_N + v_E\left(2\omega_e + \frac{v_E}{(N+h)\cos\varphi}\right)\sin\varphi - v_D\frac{v_N}{M+h} \\ \dot{v}_E - v_N\left(2\omega_e + \frac{v_E}{(N+h)\cos\varphi}\right)\sin\varphi - v_D\left(2\omega_e + \frac{v_E}{(N+h)\cos\varphi}\right)\cos\varphi \\ \dot{v}_D + v_E\left(2\omega_e + \frac{v_E}{(N+h)\cos\varphi}\right)\cos\varphi + v_N\frac{v_N}{M+h} - g \end{bmatrix} \quad (22)$$

The total angular velocity of the local-level navigation frame with respect to the inertial frame be expressed as

$$\boldsymbol{\omega}_{in}^n = \boldsymbol{\omega}_{ie}^n + \boldsymbol{\omega}_{en}^n \quad (23)$$

or

$$\boldsymbol{\omega}_{in}^n = \begin{bmatrix} \omega_e\cos\varphi + \frac{v_E}{(N+h)} \\ -\frac{v_N}{M+h} \\ -\omega_e\cos\varphi - \frac{v_E\tan\varphi}{(N+h)} \end{bmatrix} \quad (24)$$

4. Loosely-Coupled KF Integration

It is common to blend GPS and INS using different integration approaches (*i.e.*, loosely-coupled, tightly-coupled or ultra-tightly coupled; see [13]). In this paper, we confine our attention in the loosely-coupled (LC) approach, because this strategy can be used to evaluate the behavior of the inertial sensor stochastic model without any additional support during partial or complete GPS outages, which is not the case of the tightly-coupled integration, where one satellite signal available might be used to compute the Extended Kalman Filter (KF; *i.e.*, tightly-coupled uses GPS estimates of pseudoranges and Doppler determined by using satellite ephemeris data). There are two ways to implement the LC strategy: feed-forward and feed-back. The first one is used in systems that have a high-performance inertial measurement unit (IMU), as it merges the GPS/INS information, but it has no control over the error that may occur in the IMU; it basically works with an open-loop architecture. On the other hand, the feed-back includes a close loop that allows us to correct the INS error, where in the case of a GPS outage, the navigation solution will depend only on the INS, which will be corrected by its correspondent inertial sensor error model. The block diagram of the GPS/INS integration with feedback is shown in Figure 4.

In this strategy, the position and velocity obtained from the mechanization (r_{INS}^n and v_{INS}^n) are combined with the GPS, which delivers velocity and position data (r_{GPS}^n and v_{INS}^n). The residual error (δR^n and δV^n) calculated from the GPS and INS outputs is the input to the Kalman Filter (KF), where a state-space model is built with error states for navigation and IMU errors. The error states related to the IMU errors

[DOI: 10.22068/ijae.7.4.2562]

are fed back though the closed loop in order to correct the INS navigation solution. The system model for loosely-coupled approach is given by position error, velocity error and attitude error, which represent the navigation error states, *i.e.*, a total of nine states for 3D navigation. Moreover, the scale factors and bias for gyro and accelerometers are included in the IMU error states, and the number of states will depend on the stochastic model employed.

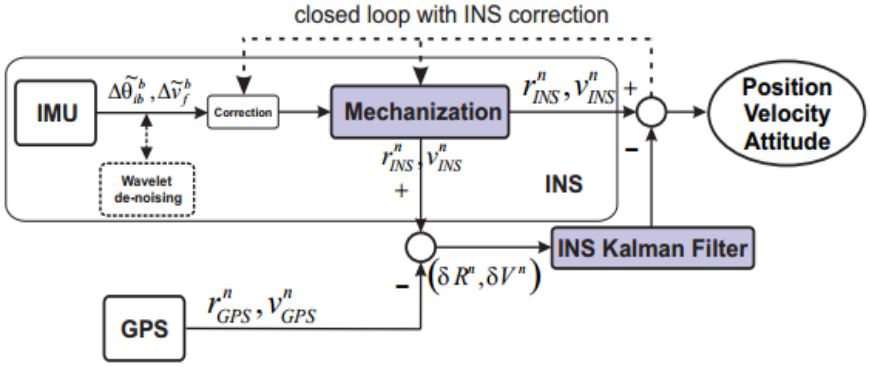

Fig4. Loosely-coupled Kalman Filter (KF) integration with feedback; figure kindly taken from []

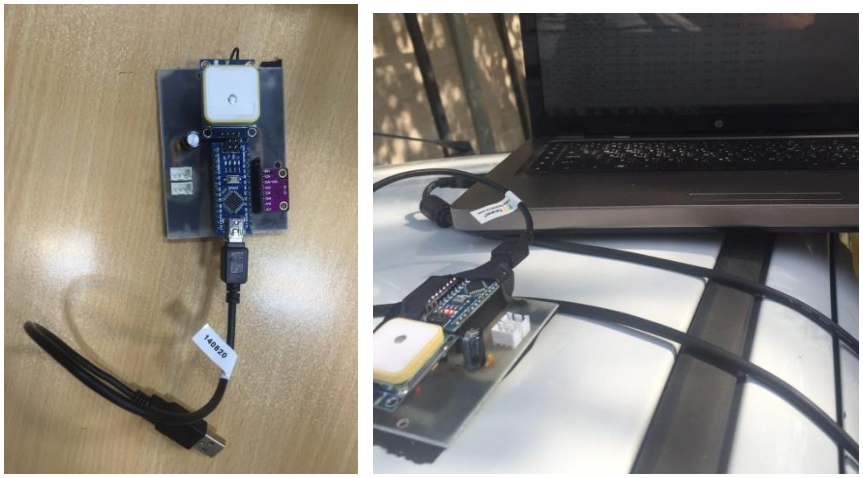

Fig5. The experimental setup

Fig6. Path of the vehicle

[DOI: 10.22068/ijae.7.4.2562]

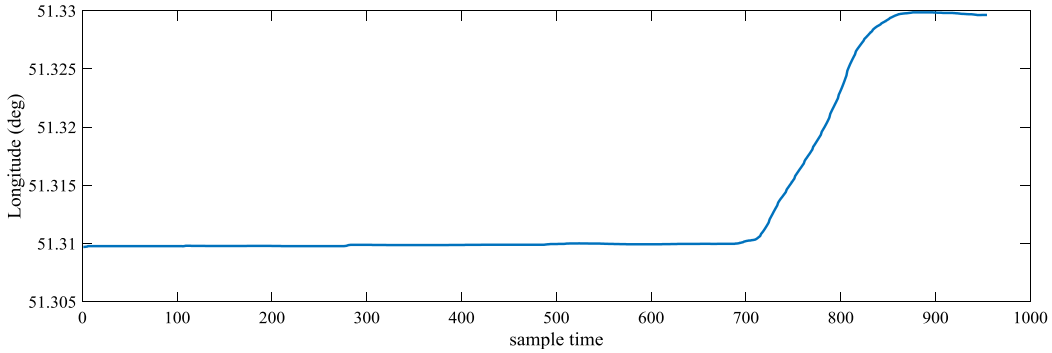

Fig7. Longitudinal of the vehicle

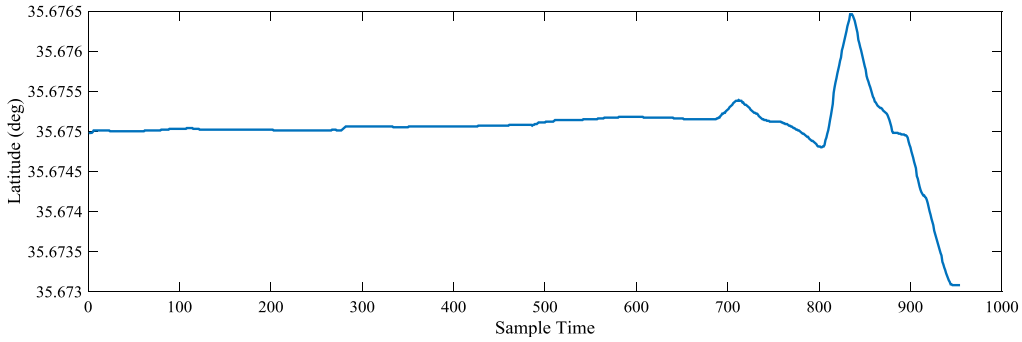

Fig8. Latitude of the vehicle

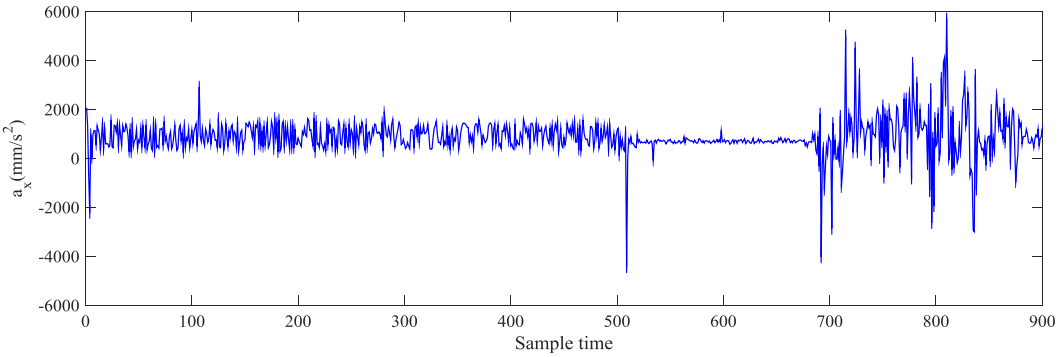

Fig9. Vehicle acceleration in X-axis

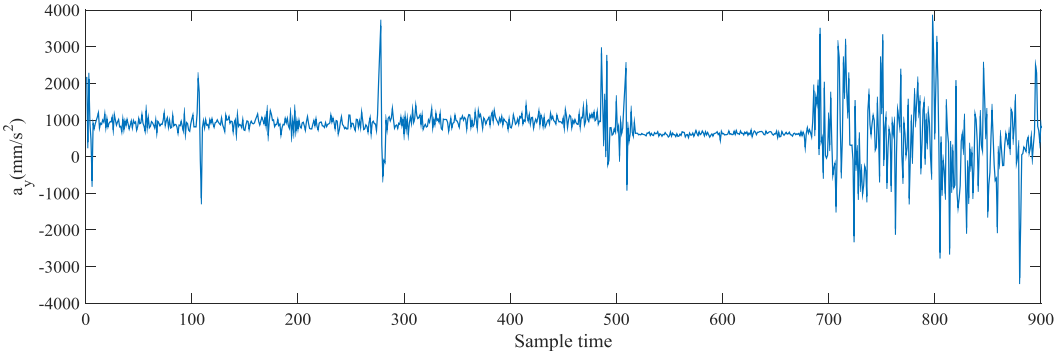

Fig10. . Vehicle acceleration in Y-axis

[DOI: 10.22068/ijae.7.4.2562]

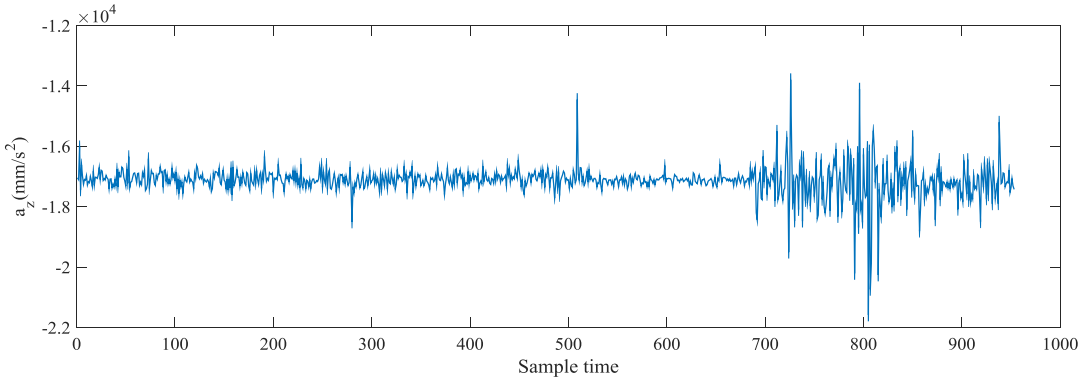

Fig11. Vehicle acceleration in Z-axis

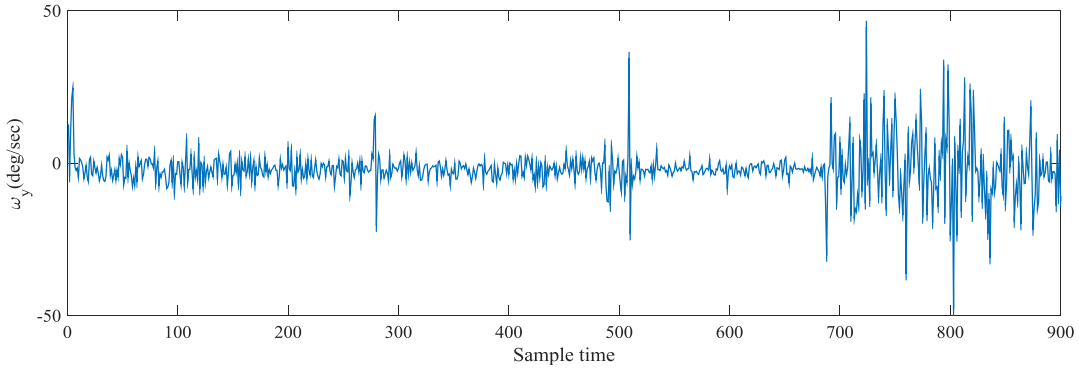

Fig12. Vehicle angular velocity in X-axis

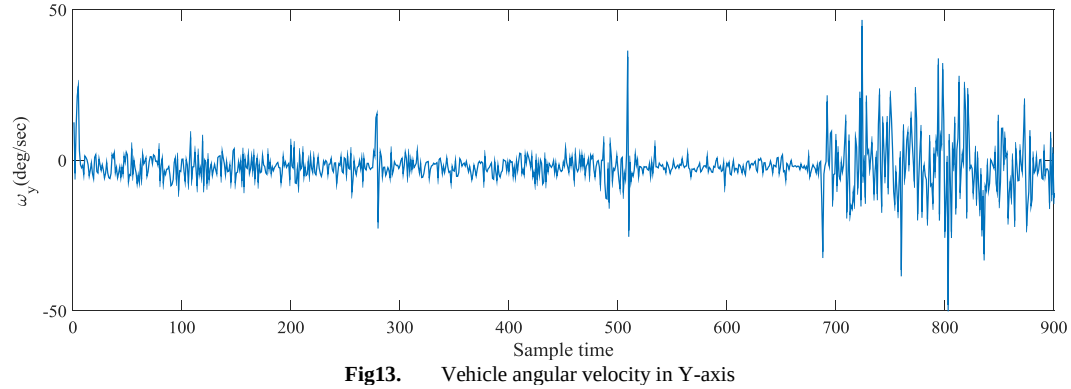

Fig13. Vehicle angular velocity in Y-axis

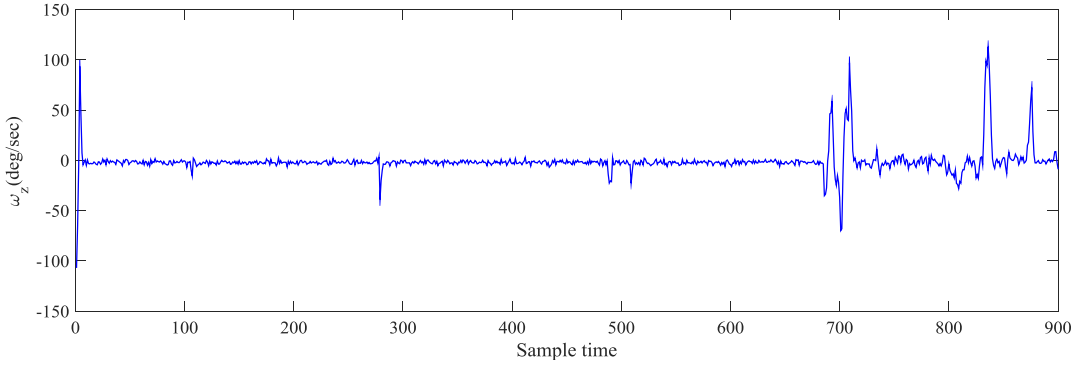

Fig14. Vehicle angular velocity in Z-axis

[DOI: 10.22068/ijae.7.4.2562]

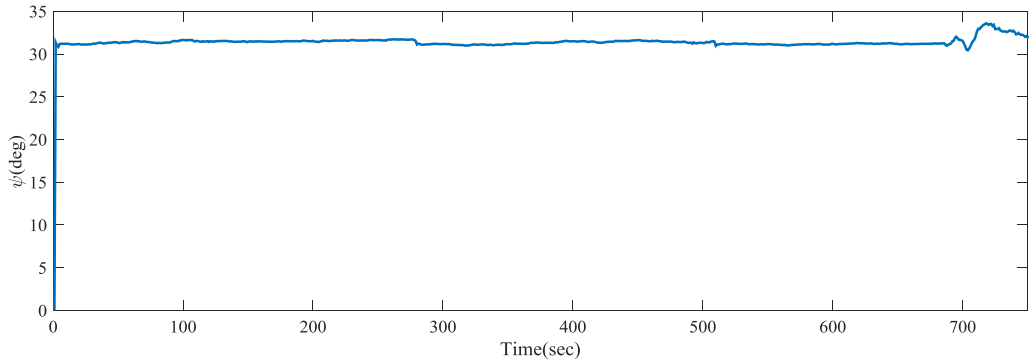

Fig15. θ angle of the vehicle

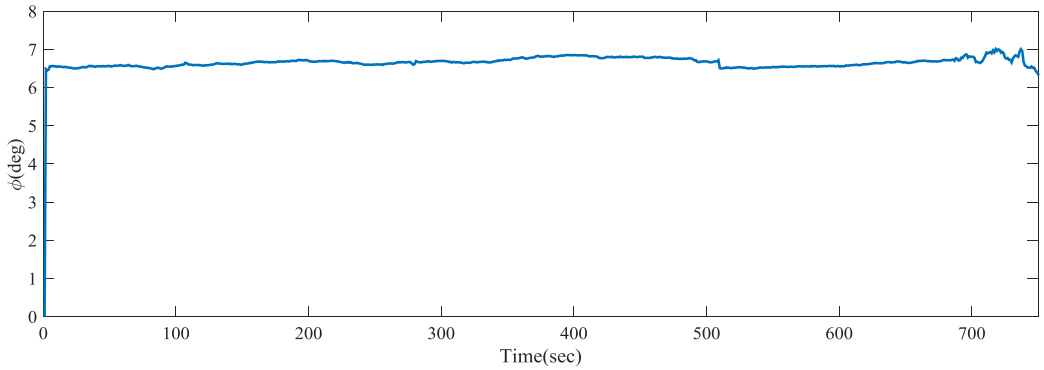

Fig16. φ angle of the vehicle

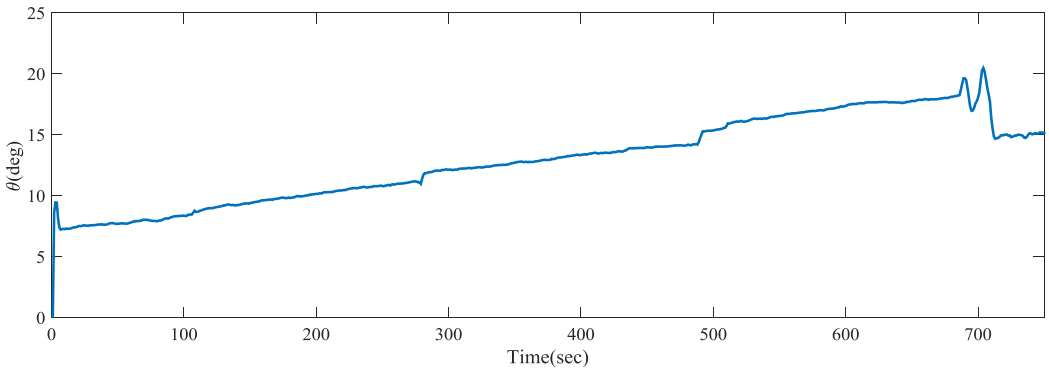

Fig17. ψ angle of the vehicle

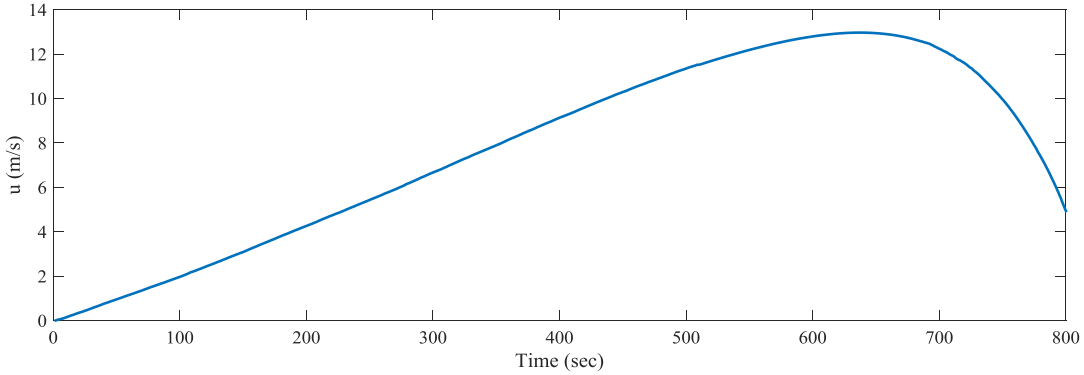

Fig18. longitudinal velocity of the vehicle

[DOI: 10.22068/ijae.7.4.2562]

5. Implementation and Experimental Results

To implement the proposed algorithm, a MPU 9250 and U-blox Neo6m have been used as an inertial measurement unit and GPS receiver, respectively. These sensors are mounted on the vehicle for navigation purposes. Figure (5) and Figure (6) show the experimental setup and path for the vehicle navigation, respectively.

The proposed data fusion algorithm has been used to estimate the position, velocity and attitude of the vehicle. Figure (7) and Figure (8) shows the longitudinal and latitude of the vehicle in the path, respectively.

The accelerations of the vehicle in XYZ inertial frame have been shown in Figure (9) to Figure (11).

Angular velocities of the vehicle in XYZ inertial frame have been shown in Figure (12) to Figure (14).

Figure (15) to Figure (17) show the attitudes of the vehicle in XYZ inertial frame.

The longitudinal velocity of the vehicle has been shown in Figure (18).

6. Conclusions

This paper has shown an effective combination of two separated systems (GPS and INS) which have their own advantages and drawbacks. The low-cost IMU is a self-obtained sensor which is not capable of determining reasonable position information. GPS, in contrast, gives good results, but is only able to calculate every single second. This paper has shown the basic integration method of GPS and INS and estimation techniques. Loosely coupled has been used for data fusion of INS and GPS. The proposed algorithm, has been tested in experimental test and the results show that this coupling method can reduce the drift in measure kinematical variables.

References

[1]. R. Zhu, D. Sun, Z. Zhou, D. Wang, A linear fusion algorithm for attitude determination using low cost MEMS-based sensors, Measurement, Vol. 40, 2007, pp. 322–328.

[2]. C.F. Kao, T.L. Chen, Design and analysis of an orientation estimation system using coplanar gyro-free inertial measurement unit and magnetic sensors, Sensors and Actuators A: Physical, Vol. 144, 2008, pp. 251–262.

[3]. D. Jurman, M. Jankovec, R. Kamnik, M. Topic, Calibration and data fusion solution for the miniature attitude and heading reference system, Sensors and Actuators A, Vol. 138, 2007, pp. 411–420.

[4]. J. Bijker, W. Steyn, Kalman filter configurations for a low-cost loosely integrated inertial navigation system on an airship, Control Engineering Practice, Vol. 16, 2008, pp. 1509–1518.

[5]. L. N. Hieu, V. H. Nguyen, Loosely Coupled GPS/INS integration with Kalman filtering for land vehicle applications, Int. Conf. Control, Automation and Information Sciences, Ho Chi Minh City, 2012, pp. 90-95.

[6]. M. Johansson, Estimation of GPS reliability and GPS/INS fusion, Master Thesis, Uppsala University, 2013.

[7]. W. Koch, Tracking and Sensor Data Fusion: Methodological Framework and Selected Applications, Springer, Berlin, 2014.

[8]. M. Tanikawara, Y. Kubo, S. Sugimoto, Modeling of sensor error equations for GPS/INS hybrid systems, Int. J. Innovative Computing, Information and Control, Vol. 6, 2010, pp. 127-138.

[9]. J. Wu, H. Zhang, Data fusion algorithm design of GPS/IMU based on fuzzy adaptive federated Kalman filter, 2nd Int. Congress on Image and Signal Processing, Tianjin, China, 2009, pp. 1-4.

[10]. C. C. M. Naranjo, Analysis and modeling of MEMS based inertial sensors, Master Thesis, KTH Electrical Engineering, Stockholm, 2008.

[11]. D. M. Mayhew, Multi-rate Sensor Fusion for GPS Navigation Using Kalman Filtering, Master Thesis, Virginia Polytechnic Institute and State University, Blacksburg, Virginia, 1999.

[12]. H. Nourmohammadi, J. Keighobadi, Decentralized INS/GNSS system with MEMS-Grade inertial sensors using QR-Factorized CKF, IEEE Sensors, Vol. 17, 2017, pp. 3278-3287.

[13]. M. A. K. Jaradat, M. F. Abdel-Hafez, Enhanced, Delay Dependent, Intelligent Fusion for INS/GPS Navigation System, IEEE Sensors, Vol. 14, 2014, pp. 1545-1554.

[DOI: 10.22068/ijae.7.4.2562]